# Effect of Protonation−Deprotonation Processes on the Electrooptical Properties of Bipyridine-Containing Poly(*p*-phenylene−vinylene) Derivatives

**Yoav Eichen,*,†,‡ Gregory Nakhmanovich,† Vladimir Gorelik,† Olga Epshtein,‡,§ Jorge M. Poplawski,‡ and Eitan Ehrenfreund‡,§**

*Contribution from the Department of Chemistry, Department of Physics, and Solid State Institute, Technion−Israel Institute of Technology, Haifa 32000 Israel*

*Received February 3, 1998*

**Abstract:** New electroluminescent, PPV-like, conjugated polymers containing bipyridylene−vinylene subunits were prepared and characterized with respect to their electrooptical properties. The polymers were found to exhibit reversible and tunable optical properties depending on protonation−deprotonation processes. pH sensitivity and reversible tunability of the polymers were observed by photo- and electroluminescence, optical absorption, photoinduced-absorption, and electroabsorption experiments. A luminescence red-shift of as much as 0.2 eV (∼60 nm) was observed upon full protonation of a free-base film. Films of the free-base form of the new polymers showed, in general, sharper spectra than the corresponding protonated films, probably due to increased disorder and stronger interchain interactions in the latter.

## I. Introduction

The discovery that poly(*p*-phenylene−vinylene) (PPV), derivatives can be used as efficient active layers in organic light-emitting diodes (OLED)[1] triggered intensive research aimed at a better understanding of the photophysics, charge transport, and optoelectronic properties of luminescent conjugated polymers.[2] Numerous studies focused on the effects of intrachain properties on the optoelectronic properties of the polymers.[3] The effects of introducing different electron-deficient and electron-rich heterocycles and the effect of tailoring specific alternating aromatic sequences on the properties of the polymers were studied extensively.[4]

Additionally, numerous studies focused on the effects of introducing different side groups to the polymer skeleton on the optoelectronic properties of the polymers.[5] In many cases, it was demonstrated that side groups, such as alkyl chains, that present only a minor direct electronic perturbation to the intrachain polymer backbone, are capable of inducing significant changes in their photophysics and electrooptics.

The photoexcited states of an isolated, nondegenerated ground state, conjugated polymer chain may include a variety of charged (polarons, bipolarons) and neutral (excitons, polaron pairs) species. In a film, interchain interactions lead to the formation of extended photoexcited species that are delocalized over more than one polymer chain, giving rise to new optical properties.[4d,f,l] The nature of the species that are delocalized over more than one polymer chain, such as neutral excimers and polaron pairs, was also studied extensively.[6]

Closely packed chains of a given polymer may form ground-state aggregates in which the electronic wave functions are delocalized over numerous polymer chains, as well as excited-state aggregates, such as excimers.[2] The influence of the packing of the polymer chains on the optoelectronic properties makes these properties dependent on film fabrication and

† Department of Chemistry.
‡ Solid State Institute.
§ Department of Physics.

(1) (a) Burroughes, J. H.; Bradley, D. D. C.; Brown, A. R.; Marks, R. N.; Medray, K.; Friend, R. H.; Burns, P. L.; Holmes, A. B. *Nature* **1990**, *347*, 539. (b) Burn, P. L.; Holmes, A. B.; Kraft, A.; Bradley, D. D. C.; Brown, A. R.; Friend, R. H. *Nature* **1992**, *356*, 47. (c) Greenham, N. C.; Morati, S. C.; Bradley, D. D. C.; Friend, R. H.; Holmes, A. B. *Nature* **1993**, *365*, 628. (d) Berggren, M.; Inganas, O.; Gustafsson, G.; Rasmusson, J.; Anderson, M. R.; Hjertberg, T.; Wennersstrom, O. *Nature* **1994**, *372*, 444. (e) Pei, Q.; Yu, G.; Zhang, C.; Yang, Y.; Heeger, A. J. *Science* **1995**, *269*, 1086. (f) Blatchford, J. W.; Epstein, A. J. *Am. J. Phys.* **1996**, *64*, 120 and references therein. (g) Gustafsson, G.; Cao, Y.; Treacy, G. M.; Klavetter, F.; Colaneri, N.; Heeger, A. J. *Nature* **1992**, *357*, 628, 1992. (h) Burroughes, J. H.; Jones, C. A.; Friend, R. H. *Nature* **1988**, *335*, 137. (i) Garnier, F.; Hajlaouni, R.; Yassar, A.; Srivastava, P. *Science* **1994**, *265*, 1684.

(2) (a) Ziemelis, K. E.; Hussain, A. T.; Bradley, D. D. C.; Friend, R. H.; Ruhe, J.; Wegner, G. *Phys. Rev. Lett.* **1991**, *17*, 2231. (b) Friend, R. H. In *Proceedings of the 81th Nobel Symposium*; Salaneck, W. R., Lundstrom, I., Ranby, B. Eds.; Oxford University Press: Oxford, U.K., 1993; pp 285−323,. (c) Heeger, A. J. In *Proceedings of the 81th Nobel Symposium*; Salaneck, W. R., Lundstrom, I., Ranby, B., Eds.; Oxford University Press: Oxford, U.K., 1993; pp 27−62. See also the following proceedings of the international conference on synthetic metals held in Seoul Korea (1994) and Snowbird, UT (1996): *Synth. Met.* **1994**, *69*−*71*, **1996**, *84*−*86*. (d) Wang. Y. Z.; Gebler, D. D.; Lin, L. B.; Blatchford, J. W.; Jessen, S. W.; Wang, H. L.; Epstein, A. J. *Appl. Phys. Lett.* **1996**, *68*, 894. (e) Onoda, M.; MacDiarmid, A. G. *Synth. Met.* **1997**, *91*, 307. (f) Chen, L. X.; Jenekhe, S. A. *Synth. Met.* **1997**, *85*, 1431. (g) Andersson, M. R.; Berggren, M.; Olinga, T.; Hjertberg, T.; Inganas, O.; Wennerstrom, O. *Synth. Met.* **1997**, *85*, 1383. (h) Granstrom, M.; Berggren, M.; Inganas, O.; Andersson, M. R.; Hjertberg, T.; Wennerstrom, O. *Synth. Met.* **1997**, *85*, 1193. (i) Rothberg, L. B.; Yan, M.; Fung, A. W. P.; Jedju, T. W.; Kwock, E. W.; Galvin, M. E. *Synth. Met.* **1997**, *84*, 537. (j) Wang, Y. Z.; Gebler, D. D.; Fu, D. K.; Swager, T. M.; MacDiarmid, A. G.; Epstein, A. J. *Synth. Met.* **1997**, *85*, 1179. (k) Bredas, J. L.; Cornil, J.; Heeger, A. J. *Adv. Mater.* **1996**, *8*, 447. (l) Soos, Z. G.; Galvao, D. S.; Etamad, S. *Adv. Mater*. **1994**, *6*, 280.

(3) (a) Bredas, J. L. *J. Chem. Phys.* **1985**, *82*, 3808. (b) Brivio, G. P.; Mulazzi, E. M. *Chem. Phys. Lett.* **1983**, *95*, 555. (c) Roncali, J. *Chem. Rev.* **1992**, *92*, 711. (d) Heeger, A. J.; Kivelson, S.; Schrieffer, J. R.; Su, W. P. *Rev. Mod. Phys.* **1988**, *60*, 781. (e) Grem, G.; Leditzky, G.; Ullrich, B.; Leising, G. *Adv. Mater.* **1992**, *4*, 36. (f) Gettinger, C. L.; Heeger, A. J.; Drake, J. M.; Pine, D. J. *Mol. Cryst. Liq. Cryst.* **1994**, *256*, 507. (g) McBranch, D.; Long, F. H.; Hagler, T. W.; Robinson, J. M.; Swanson, B. I.; Pakbaz, K.; Heeger, A. J.; Schrieker, S.; Wudl, F. *Mol. Cryst. Liq. Cryst.* **1994**, *256*, 499.

S0002-7863(98)00383-7 CCC: $15.00 
Published on Web 09/25/1998

history,[4d,l] as well as on the presence of various guest molecules capable of interacting with the polymer backbone and altering its packing patterns[4e,i,7].

Recent findings on poly(pyridylene−vinylene) derivatives suggest that their electrooptical properties may be tuned by coordination of different guest species to the lone pairs of the nitrogen atoms of the pyridine rings.[4,7,8]. Reversibility of optoelectronic properties induced by reversible changes in polymer chain packing represents an interesting phenomenon both from the scientific and technological points of view.

The present paper deals with the role of protonation−deprotonation (P−DP) processes in controlling the optoelectronic properties of PPV-like polymers containing 2,2′-bipyridylene−vinylene subunits. We have found that, upon protonation of the "pristine" form of the polymer, the optical gap decreases substantially. This reduction of the gap was observed in photo- and electroluminescence, absorption, photoinduced absorption, and electroabsorption. The P−DP process was reversible, and the color could be changed continuously between yellow and red depending on the degree of protonation, without measurable degradation during more then 10 cycles. It is also found that, upon protonation, the interchain interactions are significantly increased.

## Experimental Section

**a. Materials.** Synthesis and analytical data regarding the different monomers and polymers are described in the Supporting Information section.

**b. Preparation of Samples.** Films for absorption, photoinduced absorption, and photoluminescence measurements were prepared by spin coating glass or quartz substrates with the appropriate polymer from formic acid solutions, followed by oven-drying (70 °C, $10^{-5}$ mmHg, 120 h). This procedure yielded reproducible and homogeneous, 50−100-nm-thick films, according to the frequency of the spinner and the concentration of the polymer solution. Samples for electroabsorption measurements were prepared using a similar spin-coating process on quartz substrates bearing two interdigitated electrodes, 20 $\mu$m apart. Electroluminescent devices were prepared by spin coating the polymer on an indium tin oxide (ITO)-coated glass. Aluminum electrodes (20 $mm^2$, typically 100 nm thick) were deposited on the oven-dried films using standard CVD techniques.

**c. Apparatus.** Film thickness was determined using an α-Step (Tencor Inst. α-Step 200). Absorption spectra were measured using a Cary 1E (Varian) spectrophotometer. Photoluminescence (PL) and electroluminescence (EL) spectra were recorded on a PC-controlled, homemade, spectrometer consisting of a pulsed Nd:YAG laser (Continuum, Powerlight, third harmony, 355 nm), a stabilized power supply, and a detection system consisting of a liquid nitrogen-cooled CCD (Princeton Instruments) connected to a 150*i*-mm spectrograph (Acton Research). A liquid nitrogen-cooled optical cryostat (Oxford, Instrument, DN 1704) equipped with a temperature controller (Lake Shore 330, Cryotronics) was used to regulate the temperature of the samples. A homemade sample holder equipped with a gas chamber was used for measuring HCl-dependent absorption and PL spectra. First, the chamber was evacuated and then dry HCl gas was transferred into the chamber via a syringe. Dry nitrogen was added to the chamber to adjust pressure to 1 atm. Spectra of the polymers were taken at different time intervals after the injection in order to ensure data acquisition at equilibrium. Data presented in this paper correspond to systems in equilibrium.

Photoinduced absorption (PIA) and electroabsorption (EA) measurements were recorded on a homemade spectrometer. For PIA experiments, an argon ion laser (Coherent, Inova 70, 458 nm or all UV lines) or a 250-W xenon arc lamp was used as the pump beam and a tungsten lamp (Oriel) or a Nernst glower was used as the probe beam (for the visible−NIR and IR, respectively). EA measurements were performed by applying a modulated electric field to the sample via two interdigitated gold electrodes 20 $\mu$m apart, mounted on the quartz substrate using standard photolithography techniques. The probe light in both experiments was analyzed using various detectors (covering the UV−visible-IR regions) attached to a monochromator (Jarrel-Ash, 0.25 m) equipped with a set of interchangeable gratings. Samples were mounted onto a coldfinger cryostat (Air-Product, LT-3-1100) in a vacuum. Transmission, T, and audio frequency photomodulated transmission, $\Delta T$, were recorded using a standard phase-sensitive lock-in technique. The ratio $-\Delta T/T$ is the net change in the absorption due to the modulated pump light source (in the PIA experiment) or due to the external electric field (in the EA experiment).

## Results and Discussion

**a. Photoluminescence and Electroluminescence.** Polymers *p*-PBV, RT*p*-PBV and T*p*-PBV were prepared according to Scheme 1. All three polymers are linear PPV derivatives that contain 5,5′-vinylene-2,2′-bipyridine units in their backbone. The new polymers were insoluble in conventional organic solvents, including their polymerization solutions from which they separated as bright yellow precipitates. The new polymers were readily soluble in formic acid, yielding dark orange, highly luminescent solutions. Evaporation of solvent yielded uniform and robust orange films having orange-red luminescence. Figure 1 presents the PL spectra of *p*-PBV in formic acid at different

(4) (a) Yamamoto, T.; Shimura, M.; Osakada, K.; Kubota, K. *Chem. Lett.* **1992**, 1003. (b) Zhou, Z. H.; Maruyama, T.; Kanbara, T.; Ikeda, T.; Ichimura, K.; Yamamoto, T.; Tokuda, K. *J. Chem. Soc., Chem. Commun.* **1991**, 1210. (c) Nakhmanovich, G.; Poplawski, J. M.; Yan S.; Gorelik, V.; Eichen, Y.; Ehrenfreund, E. *Synth. Met.* **1997**, *84*, 883. (d) Blatchford, J. W.; Jessen, S. W.; Lin, L. B.; Gustafson, T. L.; Fu, D. K.; Wang, H. L.; Swager, T. M.; MacDiarmid, A. G.; Epstein, A. J. *Phys. Rev.* **1996**, *B54*, 9180. (e) Marsella, M. J.; Fu, D. K.; Swager, T. M. *Adv. Mater.* **1995**, *7*, 145. (f) Blatchford, J. W.; Gustafson, T. L.; Epstein, A. J.; Vanden Bout, D. A.; Kerimo, J.; Higgins, D. A.; Barbara, P. F.; Fu, D. K.; Swager, T. M.; MacDiarmid, A. G. *Phys. Rev.* **1996**, *B54*, R3683. (g) Blatchford, L. B.; Gustafson, T. L.; Epstein, A. J. *J. Chem. Phys.* **1996**, *105*, 9214. (h) Blatchford, J. W.; Jessen, S. W.; Lin, L. B.; Lih, J. J.; Gustafson, T. L.; Epstein, A. J.; Fu, D. K.; Marsella, M. J.; Swager, T. M.; MacDiarmid, A. G.; Yamaguchi, S.; Hamaguchi, H. *Phys. Rev. Lett.* **1996**, *76*, 1513. (i) Fu, D. K.; Xu, B.; Marsella, M. J. *Polym. Prepr. (Am. Chem. Soc. Div. Polym. Chem.)* **1995**, *36*, 586. (j) Gebler, D. D.; Wang, Y. Z.; Blatchford, J. W.; Jessen, S. W.; Lin, L. B.; Gustafson, T. L.; Wang, H. L.; Swager, T. M.; MacDiarmid, A. G.; Epstein, A. J. *J. Appl. Phys.* **1995**, *78*, 4264. (k) Yamamoto, T.; Komarudin, D.; Arai, M.; Lee, B. L.; Suganuma, H.; Asakawa, N.; Inoue, Y.; Kubota, K.; Sasaki, S.; Fukuda, T.; Matsuda, H. *J. Am. Chem. Soc.* **1998**, *120*, 2047. (l) Jessen, S. W.; Blatchford, J. W.; Lin, L. B.; Gustafson, T. L.; Partee, J.; Shinar, J.; Fu, D. K.; Marsella, M. J.; Swager, T. M.; MacDiarmid, A. G.; Epstein, A. J. *Synth. Met.* **1997**, *84*, 501.

(5) (a) Dottinger, S. E.; Hohloch, M.; Segura, J. L.; Steinhuber, E.; Hanack, M.; Tompert, A.; Oelkrug, D. *Adv. Mater.* **1997**, *9*, 233. (b) Roncali, J. *Chem. Rev.* **1997**, *97*, 173. (c) McCullough, R. D.; Lowe, R E. *J. Chem. Soc., Chem. Commun.* **1992**, 70. (d) McCullough, R. D.; Lowe, R. D.; Jayaraman, M.; Anderson, D. L. *J. Org. Chem.* **1993**, *58*, 904. (e) Huang, F.; Wang, H. L.; Feldstein, M.; MacDiarmid, A. G.; Hsieh, B. R.; Epstein, A. J. *Synth. Met.* **1997**, *85*, 1283.

(6) (a) Jenekhe S. A.; Osaheni, J. A. *Science* **1994**, *265*, 765. (b) Mizes, H. A.; Conwell, E. M. *Phys. Rev.* **1994**, *B50*, 11243. (c) Lemmer, U.; Heun, S.; Mahrt, R. F.; Scherf, U.; Hopmeier, M.; Siegner, U.; Gober, E. O.; Muller, K.; Bassler, H. *Chem. Phys. Lett.* **1995**, *240*, 373.

(7) Wang, B.; Wasielewski, M. R. *J. Am. Chem. Soc.* **1997**, *119*, 12.

(8) Wang, Y. Z.; Gebler, D. D.; Fu, D. K.; Swager, T. M.; Epstein, A. J. *Appl. Phys. Lett.* **1997**, *70*, 3215.

**Scheme 1**

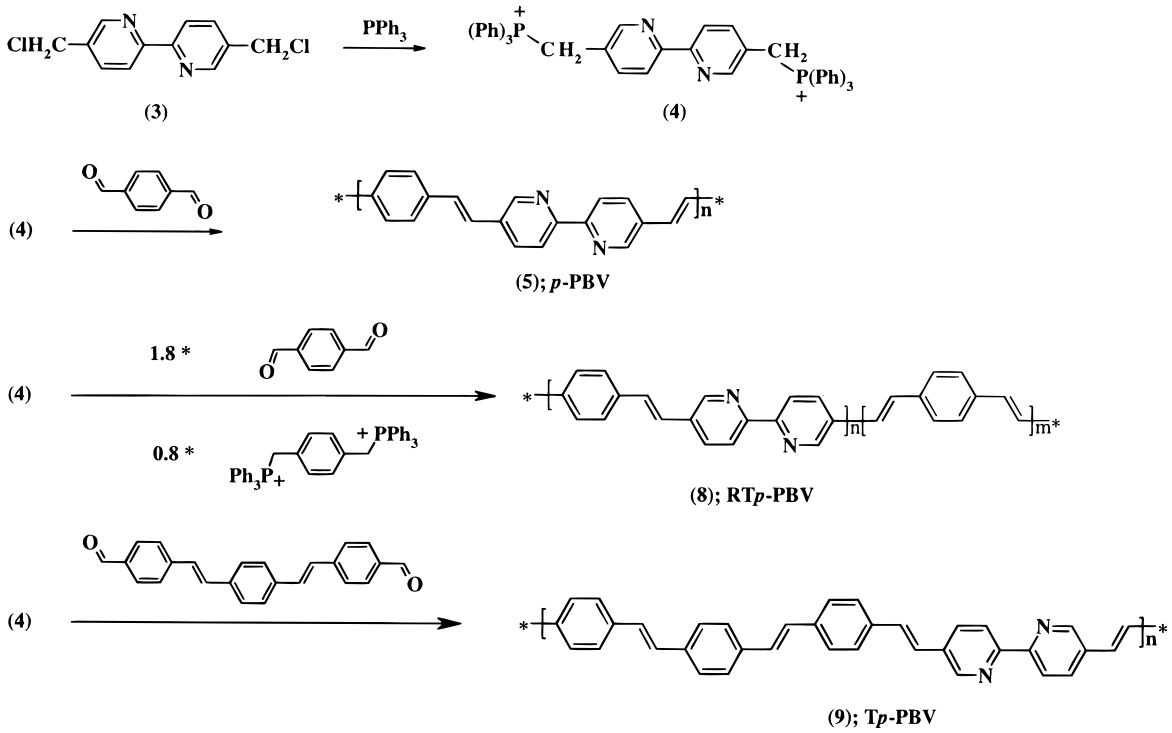


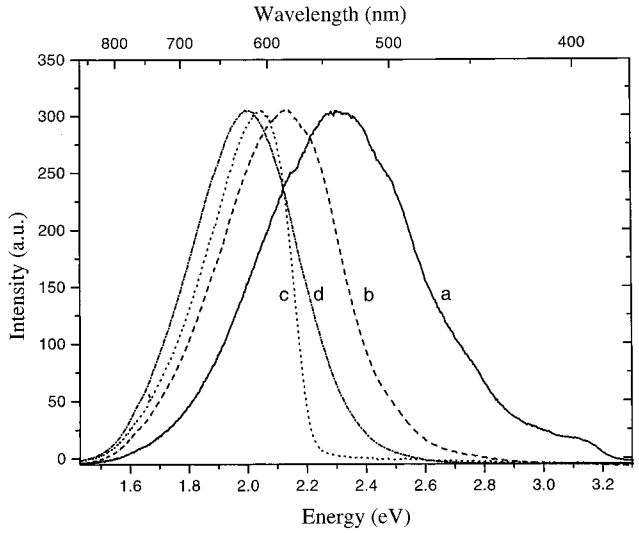


**Figure 1.** Photoluminescence spectra (normalized) of *p*-PBV: (a) a $10^{-7}$ M solution of *p*-PBV in formic acid, (b) a $10^{-5}$ M solution of *p*-PBV in formic acid, (c) a $10^{-3}$ M solution of *p*-PBV in formic acid, and (d) a film of *p*-PBV on a glass.

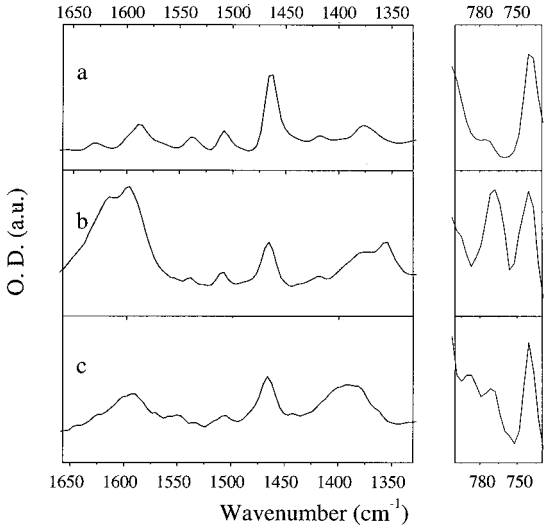


**Figure 2.** Infrared spectra of *p*-PBV: (a) pristine, (b) film obtained from a formic acid solution, after drying under vacuum ($10^{-5}$ mmHg, room temperature), and (c) after heating the film in (b) under vacuum ($10^{-5}$ mmHg, 70 °C, 120 h).

concentrations (Figure 1a−c) and the PL spectrum of a *p*-PBV film on a glass substrate (Figure 1d). Similar to other *p*-pyridylene−vinylene polymers,[2,12] the PL spectrum of *p*-PBV in formic acid solutions is concentration-dependent, indicating the formation of aggregates (in the ground or excited state) at higher concentrations. The PL spectrum of the film is similar to the one obtained from concentrated solutions of *p*-PBV in formic acid. Both in films and in concentrated solutions, the close packing of the polymer chains increases the interchain exciton interactions, thus giving rise to a significant red-shift. Figure 2 displays the IR spectra of a *p*-PBV film: (a) in its pristine form, (b) after casting it from formic acid (vacuum-dried, $10^{-5}$ mmHg, room temperature, 12 h), and (c) after heating the sample under vacuum ($10^{-5}$ mmHg, 70 °C, 120 h), respectively. The IR spectra of polymer films that have been obtained from formic acid solutions show the indicative absorption bands of formate ions at 1616, 1354, and 768 $cm^{-1}$. Comparison of the relative intensities of the formate bands with the vinylene bands at 961 $cm^{-1}$ (not shown) yields an estimated ratio of $[HCOO^-]/[N] = 1.5 \pm 0.5$ under saturation conditions. Exposure of a powder sample of the polymer to HCl vapors resulted in a clear change in its elemental analysis composition with a ratio of $[HCl]/[N] = 1 \pm 0.05$ (see Supporting Information). Heating the polymer film under reduced pressure ($10^{-5}$ mmHg, 70 °C) results in a gradual disappearance of the formate absorption bands in the IR spectrum, Figure 2c. The IR spectrum of the film after 120 h ($10^{-5}$ mmHg, 70 °C) is practically identical to the IR spectrum of the pristine polymer.

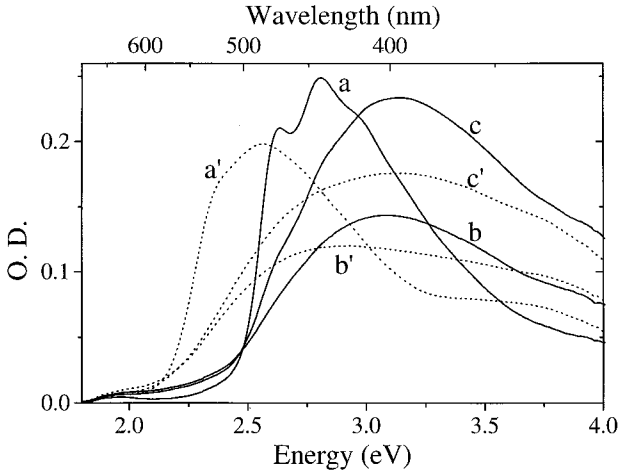


**Figure 3.** Absorption spectra of thin films of the different polymers in their free-base and acid-saturated forms: (a) free-base form of *p*-PBV, (a′) acid-saturated form of *p*-PBV, (b) free-base form of RT*p*-PBV, (b′) acid-saturated form of RT*p*-PBV, (c) free-base form of T*p*-PBV, and (c′) acid-saturated form of T*p*-PBV.

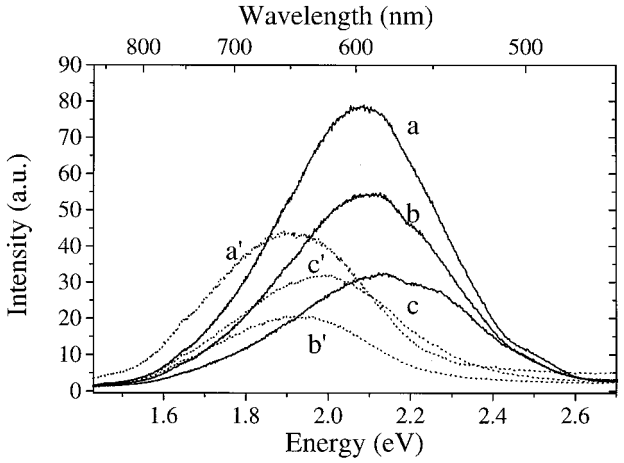


**Figure 4.** PL spectra of thin films of the polymers in their free-base and acid-saturated forms, $\lambda_{excitation} = 355$ nm: (a) free-base form of *p*-PBV, (a′) acid-saturated form of *p*-PBV, (b) free-base form of RT*p*-PBV, (b′) acid-saturated form of RT*p*-PBV, (c) free-base form of T*p*-PBV, and (c′) acid-saturated form of T*p*-PBV.

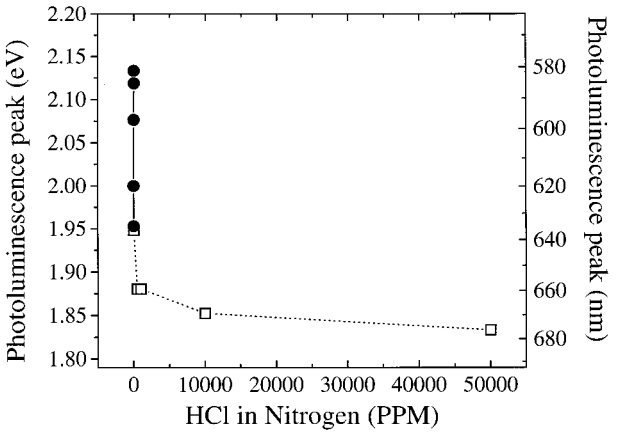


**Figure 5.** Dependence of the PL peak of a *p*-PBV film, diameter = 25 mm, on the concentration of HCl in its ambient atmosphere ($N_2$), $V = 1$ L. $\lambda_{excitation} = 355$ nm.

Reexposing the polymer film to formic acid vapors results in the reappearance of the formate bands in the IR spectrum (not shown), indicating that, under our experimental conditions, the acid induced process is reversible.

Heating the polymer film results in a gradual change of color from orange to yellow-green as well as a change in the color of the luminescence, from orange-red (acidic form) to yellow (free base). The absorption and emission spectra of the different polymer films are extremely sensitive to the presence of even minute traces of acidic or basic vapors in their surrounding atmosphere. Figure 3 presents the absorption spectra of films of the three polymers in their free-base and acid-saturated forms. The absorption spectra of free-base polymers peak at 2.8 (443 nm), 3.08 (403 nm), and 3.15 eV (394 nm) for *p*-PBV, RT*p*-PBV, and T*p*-PBV, respectively. Upon exposing the films to dry HCl vapors in nitrogen, the absorption maximum shift to 2.56 (484 nm), 2.84 (437 nm), and 3.11 eV (399 nm), respectively, presenting P−DP-induced shifts of 0.24 (49 nm), 0.24 (34 nm), and 0.04 eV (5 nm) for the respective polymers. Films that were exposed to acid vapors are stable at ambient temperatures and revert to their free-base state by thermal annealing. The same effect could be generated by exposing the polymers to vapors of various bases such as ammonia and triethylamine, indicating that the process is a simple P−DP process rather than reaction of the aromatic skeleton. The P−DP cycle is highly reversible and can be repeated without any notable degradation of the film and its optical properties for at least 10 times.

Figure 4 shows the PL spectra of the three polymers in their free-base and acid-saturated forms. The PL spectra of free-base films peak at 2.14 (580 nm), 2.14 (580 nm) and 2.15 eV (578 nm) for polymers *p*-PBV, RTp-PBV, and T*p*-PBV, respectively. Upon exposure to dry HCl vapors in nitrogen atmosphere, the absorption maximum shift to 1.94 (640 nm), 1.95 (635 nm), and 1.98 eV (627 nm), respectively. This represents P−DP-induced shifts of 0.20 (60 nm), 0.19 (55 nm), and 0.17 eV (49 nm) for the respective polymers.

Figure 5 presents the dependence of the PL maximum on the concentration of HCl in the ambient atmosphere for a film of *p*-PBV. The response curve of $\lambda_{max}$ of the PL as a function of HCl vapor concentration consists of two different domains. At low HCl concentrations, the polymer reacted irreversibly and the observed spectral shifts are not changed upon exposure to ambient atmosphere at room temperature. Deconvolution of intermediate PL bands in the irreversible part of the titration curve reveals that they constitute of two, partially overlapping, bands of the free-base (peak at 580 nm) and fully protonated (peak at 640 nm) species (see Supporting Information). At higher concentrations, a new band develops at 670 nm, contributing to a further shift of the overall luminescence band. The latter band disappears spontaneously when the vapor pressure of the HCl gas is lowered.

Panels a and b of Figure 6 display the temperature dependence of the photoluminescence spectra of free-base and acid-saturated *p*-PBV films, respectively. The insets in the figures show the dependence of the inverse integrated luminescence vs inverse temperature. This dependence was fitted using a model that takes into account deactivation of the luminescent excitons via three channels, namely, (a) luminescence, (b) one dominant thermally activated process, and (c) a temperature-independent process. According to this model, the PL intensity, $I_{PL}$, can be written as

$$1/I_{PL} = a + b\mathrm{e}^{-E_a/RT} \qquad (1)$$

where *a* and *b* are the relative probabilities for the temperature-

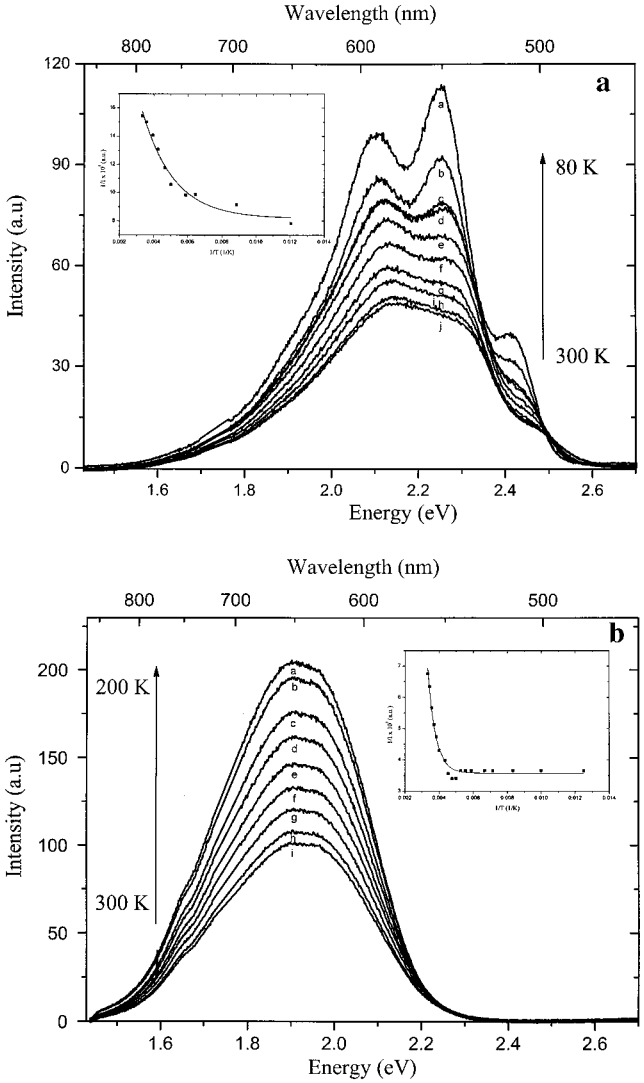


**Figure 6.** 6 (a) Temperature dependence of the luminescence spectra of the free-base form of a *p*-PBV film: (a) 83, (b) 113, (c) 155, (d) 170, (e) 200, (f) 215, (g) 235, (h) 253, (i) 280, and (j) 300 K. The inset shows the dependence of the inverse integrated emission vs inverse temperature. (b) Temperature dependence of the luminescence spectra of the acid-saturated form of a *p*-PBV film: (a) 83−210, (b) 220, (c) 230, (d) 250, (e) 260, (f) 270, (g) 280, (h) 290, and (i) 300 K. The inset shows the dependence of the inverse integrated emission on inverse temperature.

independent and temperature-dependent relaxation paths, respectively, and $E_a$ is the activation energy for the thermally activated process. The solid lines in the insets of Figure 6 are the fits of eq 1 to data. Interestingly, the increase in the barrier of the activated process in the excited state, $\Delta E = 0.14 \pm 0.02$ eV ($E_{a(\text{free base})} = 0.046 \pm 0.007$ eV, $E_{a(\text{acid satd})} = 0.19 \pm 0.016$ eV), and the observed bathochromic shift in the PL spectrum ($\Delta E = 0.20 \pm 0.02$ eV) are similar. A possible explanation to this observation is that most of the effect originates from lowering of the luminescent excited state in the protonated form (Scheme 2).

For comparison, the PL properties of a short oligomer analogue, **7**, of the new polymers was investigated. Figure 7

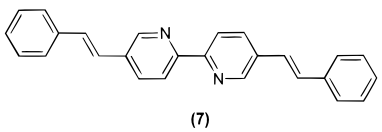


(7)

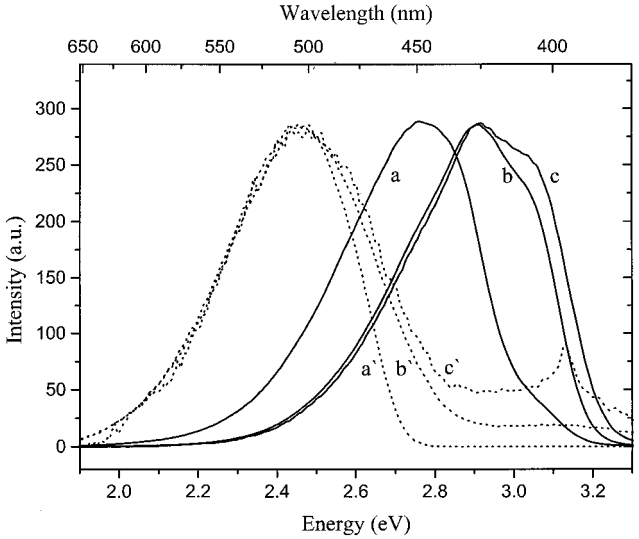


**Figure 7.** PL spectra of free-base (solid lines) and protonated (dotted lines) **7** in ethanol solutions as a function of the concentration: (a) A saturated solution, (b) $10^{-3}$ M, and (c) $10^{-7}$ M. The curves are normalized for clarity.

**Scheme 2**

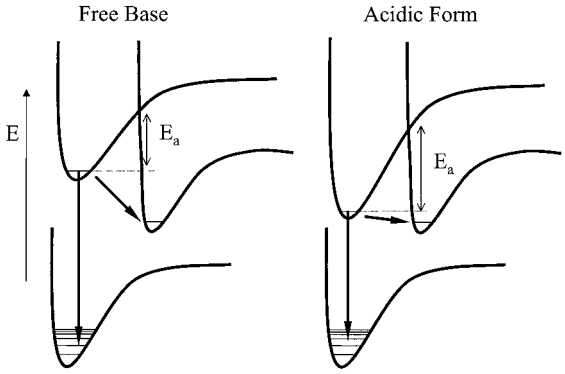


shows the PL spectra of free base and protonated **7** in ethanol solutions at different concentrations. Solutions of **7** display P−DP-dependent PL characteristics that are similar to the ones observed for the three polymers, irrespective of the nature of the solvent and over a wide range of concentrations. This indicates that at least part of the observed P−DP effect originates from changes in the electronic properties of the substance at the molecular level. However, at the higher concentration regime, a further bathochromic shift is observed due to aggregation phenomena and supramolecular interactions.

Figure 8 depicts the PL spectra of a thin film of *p*-PBV after exposure to different acidic vapors. The bathochromic shift in the PL spectrum seems to depend mainly on the strength of the acid, while the relative intensity of the PL seems to depend mainly on the redox properties of the anion. For example, the PL of a film of *p*-PBV that was exposed to formate vapors is shifted from 580 to 610 nm. This shift is accompanied by only minor quenching of the PL $I_{\text{acid form}}$:$I_{\text{free base}} = 0.9 \pm 0.1$. Exposing the same film to hydrogen iodide or nitric acid vapors results in a complete quenching of the PL.

Both free-base and protonated polymers show relatively intense EL. Figure 9 displays the EL spectra obtained from films of *p*-PBV after treating them with different acids/bases. The EL of a polymer film in its free-base state peaks at $\lambda_{max} = 585$ nm while the EL of identical polymer films that were exposed to formic acid and hydrochloric acid vapors peak at $\lambda_{max} = 615$ nm and $\lambda_{max} = 640$ nm, respectively. Evidently,

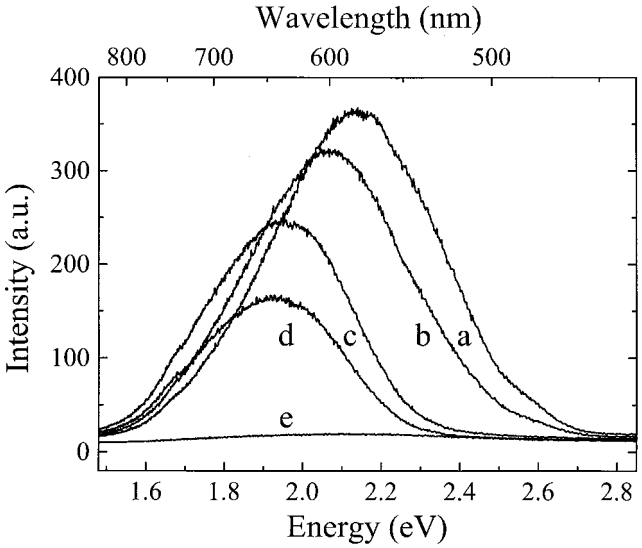


**Figure 8.** PL spectra of thin films of *p*-PBV after treatment with the following: (a) ammonia vapors, (b) as deposited from formic acid, (c) hydrochloric acid vapors, (d) hydrobromic acid vapors, and (e) hydroiodic acid vapors.

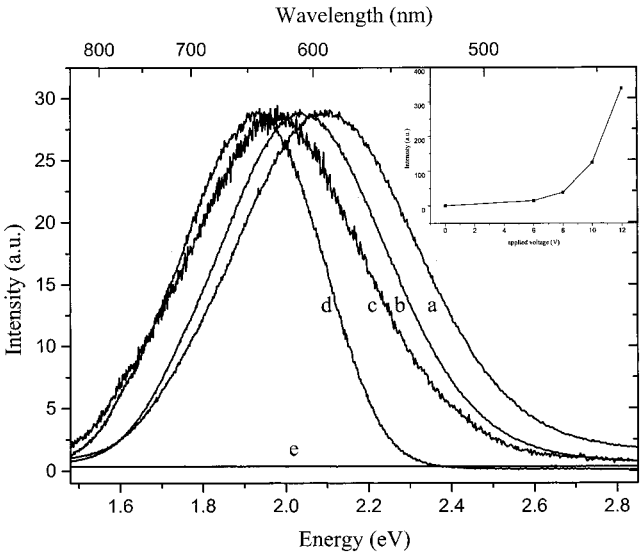


**Figure 9.** EL spectra of thin films of *p*-PBV after treatment with the following: (a) ammonia vapors, (b) as deposited from formic acid, (c) short exposure to hydrochloric acid vapors, and (d) hydrochloric acid vapors. Curve e shows the EL spectrum of each of the samples under reversed bias of −10 V. The curves are normalized for clarity. The inset shows the integrated EL intensity of a film of *p*-PBV, obtained from formic acid solutions, as a function of the applied bias.

the EL of a film can be tuned over the yellow to deep-red spectral range simply by exposing it to different acid/base conditions prior to the deposition of electrodes. The EL of various devices based on the *p*-PBV polymer at its different protonation states sets on at ∼6−7 V. The inset in Figure 9 depicts the integrated intensity of the EL of a film of *p*-PBV, obtained from formic acid solutions, as a function of the applied bias.

The packing-dependent interchain interactions are observed also in the PIA and EA spectra as shown below.

**b. Photoinduced Absorption.** Figure 10 shows the PIA spectra of acid-saturated (solid line) and free-base (broken line) films of *p*-PBV in the 0.11−2.8-eV energy range at 116 K. Both spectra are composed of an absorption region at low energies and a bleaching region at higher energies. The crossover energy

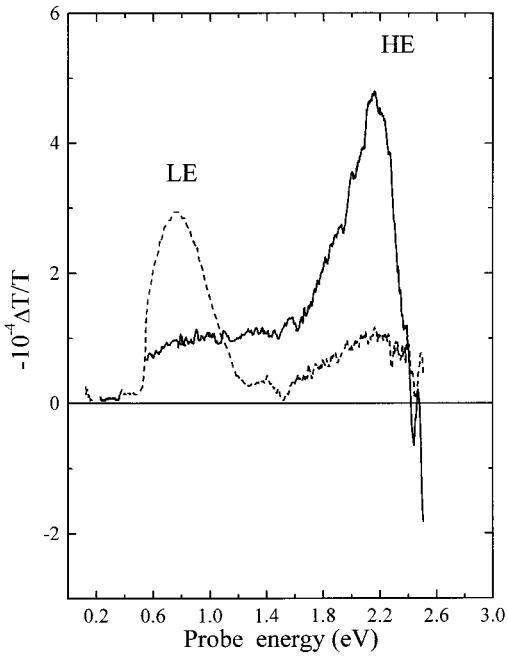


**Figure 10.** PIA spectra of a free-base film (broken line) and an acid-saturated film (solid line) of *p*-PBV in the 0.11−3-eV energy range at 116 K.

between the two regimes marks the optical energy gap,[9] above which oscillator strength is transferred to photoinduced in-gap states. The crossover energy for the *p*-PBV film treated with HCl gas is at ∼2.4 eV while that of the free-base film is situated at ∼2.6 eV. Thus, the crossover energy is red-shifted upon protonation by as much as 0.2 eV. Below the crossover energy, the two films show very different photoinduced absorption spectra. In the free-base film there appear a relatively strong low-energy (LE) band at ∼0.75 eV and a much weaker and wider high-energy (HE) band covering the 1.8−2.5-eV region. No absorption due to photoinduced infrared-active vibrations (IRAV), characteristic of charged excitons, were observed. This indicates that the LE and HE bands belong to neutral photoexcited species. Upon exposing the film to HCl vapors, the HE band becomes stronger and sharper, having a pronounced peak at ∼2.15 eV while the LE band almost disappears. PIA experiments performed on a *p*-PBV film exposed to increasing amounts of HCl vapors show a gradual evolution of the PIA spectrum starting from the spectrum of the free-base form and ending with the spectrum of the protonated form. The different spectra differ in the ratio between the intensities of the LE and HE bands at each degree of protonation. The two bands display different temperature dependence and different modulation frequency dependence. Thus, the LE and HE bands must have different origins. It appears that the species responsible for LE are more stable in the base form, while those responsible for HE are more stable in the disordered acid form. These bands may possibly originate from two different triplet excitons,[10,11] one characteristic to the fully protonated form and the other to the fully deprotonated form. However, the exact identification of these bands must await further study.

(9) (a) Vardeny, Z.; Tauc, J. *Phys. Rev. Lett.* **1985**, *54*, 1844. (b) Vardeny, Z.; Ehrenfreund, E.; Brafman, O.; Nowak, M.; Schaffer, H.; Heeger, A. J.; Wudl, F. *Phys. Rev. Lett.* **1986**, *56*, 671.

(10) (a) Janssen, R. A. J.; Moses, D.; Sariciftci, N. S. *Mol. Cryst. Liq. Cryst.* **1994**, *256*, 487. (b) Lane, P. A.; Wei, X.; Vardeny, Z. V.; Poplawski, J.; Ehrenfreund, E.; Ibrahim, M.; Frank, A. J. *Synth. Met.* **1996**, *76*, 57.

(11) Ruhe, J.; Colinari, N. F.; Bradley, D. D. C.; Friend, R. H.; Wegner, G. *J. Phys: Condens. Matter* **1990**, *2*, 5465.

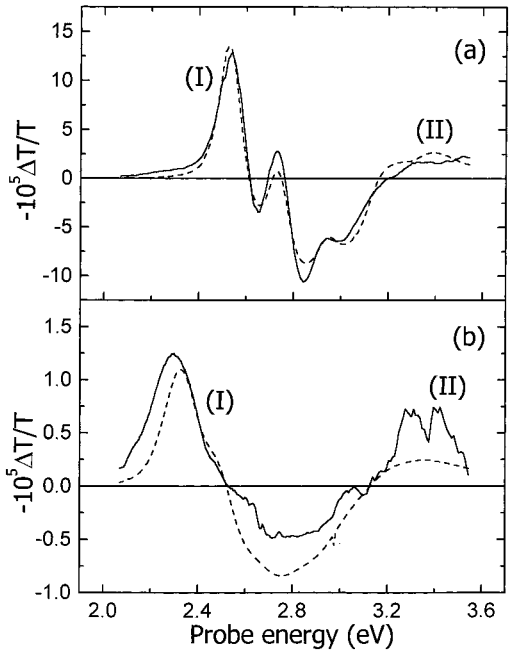


**Figure 11.** EA spectra of free-base (a) and acid-saturated (b) films of *p*-PBV at 100 K and at an electric field of $E = 10^5$ V·cm$^{-1}$. The dashed lines represent the fit to data as explained in the text.

In a previous investigation of similar pyridine-based polymers,[4l] two absorption bands at 1.8 and 0.9 eV were found in the PIA at the millisecond time regime. The authors assigned the HE peak at 1.8 eV to a triplet−triplet transition and the LE peak to polarons. The authors attributed the varying ratios between these two peaks in samples that were prepared in different ways to the formation of different aggregation states in the different samples.

**c. Electroabsorption.** Panels a and b of Figure 11 depict the EA spectra of free-base and fully protonated films of *p*-PBV, respectively, in the energy range of 2.1−3.6 eV, at 100 K and at $F = 10^5$ V·cm$^{-1}$. Spectra taken at various electric fields revealed that the EA response is proportional to $F^2$, showing the dominance of the quadratic field term in these polymers. In the free-base film, the EA spectrum (solid line, Figure 11a) is composed of sharp features (denoted as I) near the band edge observed in the absorption spectrum (Figure 3), followed by a weaker band (denoted as II) at ∼3.3−3.4 eV. Band I is derivative-like with zero crossing at 2.62 eV, followed by three, well-resolved, vibronic satellites at 2.65, 2.83, and 3.00 eV, respectively. As analyzed by Liess et al.,[12] these features are the result of a Stark red-shifted $1B_u$ exciton energy and its phonon sidebands. These relatively sharp features are commonly observed in conjugated polymers, showing the sensitivity of the EA to the band edge. Band II, which is located considerably above the $1B_u$ exciton, is interpreted as due to an optically forbidden transition $1A_g \rightarrow mA_g$, made partially allowed by the electric field. Following Liess et al., we have used the model of Orr and Ward[13] for the third-order susceptibility, $\chi^3$, limiting the summation over states to $1B_u$ and $mA_g$, and modeled the disorder in the film by an asymmetric Gaussian distribution of the conjugation length. The distribution in conjugation lengths causes a distribution in the $1B_u$ exciton energy (the HOMO−LUMO energy gap), due to its dependence on the conjugation length. The results of the fit are shown as a dotted line in Figure 11a, giving 2.6 eV for the $1B_u$ exciton energy of the most probable conjugation length and a distribution width of ∼0.2 eV of the $1B_u$ exciton energy due to the distribution in conjugation length.

The EA spectrum of the acid-saturated film is red-shifted relative to the free-base film and is much weaker and less featured (solid line, Figure 11b). Using the same model to fit the data (dotted line, Figure 11b), we find that the distribution width of the conjugation length in the acid-saturated polymer increases to 0.4 eV and that the $1B_u$ exciton has red-shifted from 2.6 eV in the free-base film to 2.3 eV in the acid-saturated film. The increase of the distribution width of the conjugation lengths, from 0.2 eV in the free-base film to 0.4 eV in the acid-saturated film, strongly supports our suggestion that the observed spectral shifts originate from changes in the packing of the chains in the film that affect their electronic properties. The significantly wider distribution shows that, upon protonation, a considerable change in the aggregation pattern of the polymer takes place and the film becomes less ordered. These observations clearly demonstrate the role of packing in the control of the photophysical and electrooptical properties of these polymers. The observation that the free-base film is more ordered than its acid-saturated analogue is in accordance with the temperature dependence of the PL spectra (Figure 6). From the temperature dependence of the PL spectra we learn that no vibronic structure can be resolved in protonated films, even at low tempratures. This indicates the formation of a "loose" structure with many different interchain interactions, in contrast to what is observed in the free-base film, where vibronic levels are clearly observable at low temperatures.

## Conclusions

This work reports the preparation and optical characterization of a new type of electroluminescent bipyridine-containing PPV-like polymers displaying variable (EL) and tunable (PL, absorption, EA, PIA) optical properties based on protonation-−deprotonation processes. The nature of the P−DP process is investigated by diverse optical and electrical characterization techniques such as absorption, photoluminescence, electroluminescence, photoinduced absorption, and electroabsorption spectroscopic techniques. Clearly, the tunability of these novel polymers originates from a combination of changes in the intrachain ("molecular") as well as interchain ("supramolecular") electronic properties arising from a significant change in aggregation patterns upon P−DP processes. The absorption and emission spectra showed clearly that aggregation phenomena play a major role in determining the electronic properties of the films. The temperature dependence of the luminescence spectra of the acid-saturated and free-base films revealed a significant change in properties upon protonation. In contrast to the relatively sharp luminescence of the free-base films, having distinct phonon sidebands, the luminescence of the acid-saturated films was broad and lacked any vibrational structure at all temperatures. Complementary electroabsorption experiments revealed that the difference in the structure and distribution of sites is not limited to emissive species. The EA experiments clearly suggest that, in addition to the differences in the nature of the absorbing species, there is a considerable difference in the distribution of the conjugation lengths of the chromophores in the two states of the polymer. Here, too, the site distribution of the chromophores in the acid-saturated film (0.4 eV) is much larger than the distribution of chromophoric sites in the free-base film (0.2 eV). Since no covalent bond reorganization is expected to occur during P−DP processes, we

(12) Liess, M.; Jeglinski, S.; Vardeny, Z. V.; Ozaki, M.; Yoshino, K.; Ding, Y.; Barton, T. *Phys. Rev. B* **1997**, *56*, 15712.
(13) Orr, B. J.; Ward, J. F. *Mol. Phys.* **1971**, *20*, 53.

suggest that the free-base film is packed in a relatively well-defined arrangement while multiple packing patterns exist for the acid-saturated film.

We have fabricated novel photoluminescent devices, based on the above polymers, in which the color can be adjusted simply by changing the concentration of different acid/base vapors in the atmosphere surrounding the film prior to electrode deposition. Using the same approach, we have demonstrated the fabrication of different electroluminescent devices with different color emission based on the control of the aggregation state of the polymer composing the active layer.

**Acknowledgment.** This research was supported by the Israeli Ministry of Science, The ISF, administrated by the Israel Academy of Sciences and Humanities, the Fund for the Promotion of Research at the Technion, and the VPR Fund−Argentina Research Fund.

**Supporting Information Available:** Synthesis and analytical data for the different monomers and polymers (6 pages, print/PDF). See any current masthead page for ordering information and Web access instructions.

JA980383P